Quaternary Research (2024), **120**, 83–92
doi:10.1017/qua.2023.58

Research Article

Soil organic carbon induces a decrease in erodibility of black soil with loess parent materials in northeast China

Jingyi Cui[1,2], Licheng Guo[1], Shangfa Xiong[1,2], Shiling Yang[1,2], Yongda Wang[1], Shihao Zhang[1,2] and Hui Sun[3]

[1]Key Laboratory of Cenozoic Geology and Environment, Institute of Geology and Geophysics, Chinese Academy of Sciences, Beijing, 100029, China; [2]College of Earth and Planetary Sciences, University of Chinese Academy of Sciences, Beijing, 100049, China and [3]College of Geography and Environmental Sciences, Zhejiang Normal University, Jinhua, 321004, China

Abstract

Although black soil in northeast China undergoes severe erosion, the contribution of parent materials, mainly Quaternary loess and non-loess sediments, to soil erodibility remains unclear. Considering the inheritance of ferromagnetic materials by parent materials, changes in magnetic parameters can successfully determine soil erodibility on a regional scale with a close climatic background. Here, we analysed the magnetic indicators of 142 samples from the black soil horizon formed on loess and non-loess sediments, covering areas of severe and slight erosion in the region to determine the effects of parent materials on the erodibility of black soil in northeast China. Both low-frequency magnetic susceptibility and frequency magnetic susceptibility (χ_{fd}) were proportional to the decrease in erosion rate due to erosion-induced leaching of ferromagnetic materials, and the change in χ_{fd} was narrow for black soil with loess parent materials, corresponding to relatively low soil erodibility. Compared with loess, the addition of soil organic matter could stabilise soils against erosion, thereby inducing a decrease in the erodibility of black soil formed on loess. Additionally, sustainable soil management policies to protect black soil from further erosion are necessary and urgent under the pressure of maintaining high grain yields and preventing erosion in northeast China.

Keywords: Black soil, Loess, Soil erodibility, Frequency magnetic susceptibility, northeast China

(Received 9 May 2023; accepted 20 September 2023)

INTRODUCTION

Black soil, defined as Mollisol in the U.S. system of soil taxonomy or Chernozem in the Russian system (Liu et al., 2012a), is often thought to be controlled by a semihumid or humid climate with low temperatures and lush meadow vegetation cover. The import of plant litter increases the level of biomass C in the soil organic horizon. Subsequently, biomass C migrates downward to the soil humus layer (Gong et al., 2007). A thick, humus-rich, and dark-coloured soil horizon is a discernible characteristic of black soil (FAO, 2022). Owing to its inherently high fertility (expressed by its richness in well-humified organic matter), black soil is known as the food basket of the world or the "giant panda in arable land" in Asia. These fertile soils have been widely cultivated in black soil belts such as the Northeast Plain, Ukrainian Plain, Pampas Plain, and Mississippi Plain, and have made substantial contributions to global food production (FAO, 2022).

In the Northeast Plain, the grain crop yield accounts for one-fifth of the total crop yield in China (Wei and Meng, 2017). However, high-frequency tillage initially destroys the soil aggregate structure in the region, resulting in the direct loss of low-density particulate organic matter through erosion. Recently, a contour map depicting the erosion rate of black soil in northeast China revealed that the regional mean erosion rate is 2.22 mm/yr (Wang et al., 2022). Using an erosion rate of 2.22 mm/yr and an average black soil thickness of 25 cm as references, the black soil will be entirely eroded in approximately 113 yr without sustainable soil management. In 2021, the Ministry of Water Resources of China released a bulletin on soil and water conservation, revealing that black soils in northeast China face erosion in an area covering approximately 2.14×10^5 km^2, which is close to 20% of the region's total land area. Under the pressures of maintaining a high grain yield and erosion, black soil is probably unable to maintain a stable level of sustainable food production.

Hence, an evaluation of soil erosion on a regional scale was conducted to protect black soil in northeast China from further degradation. In some watersheds and sloping farmlands, the soil erosion rate was quantified using ^{137}Cs tracing, soil erodibility (the vulnerability of soil to erosion in the study; Song et al., 2005; Wang et al., 2013) was calculated using empirical equations, and the dominant agents of soil erosion were also determined. However, most existing documents from the region focus on exogenic erosive forces such as monsoons, precipitation, and human activities (e.g., Yang et al., 2003; Wang et al., 2010; Xu et al., 2010; Liu et al., 2011; Wang et al., 2013; Kong et al., 2022; Wang et al., 2022). Furthermore, the physical properties of soils (e.g., structure, texture, and aggregate) are considered to be intrinsic to analysis soil erodibility (Song et al., 2005; Wang et al., 2013).

Notably, inheritance of the parent material plays a critical role in determining the main physical and chemical properties of the overlying soil (Chesworth, 1973; Osher and Buol, 1998;

Corresponding authors: Licheng Guo; Email: guolicheng05@mail.iggcas.ac.cn; Shangfa Xiong; Email: xiongsf@mail.iggcas.ac.cn

Cite this article: Cui J, Guo L, Xiong S, Yang S, Wang Y, Zhang S, Sun H (2024). Soil organic carbon induces a decrease in erodibility of black soil with loess parent materials in northeast China. *Quaternary Research* **120**, 83–92. https://doi.org/10.1017/qua.2023.58

© The Author(s), 2023. Published by Cambridge University Press on behalf of Quaternary Research Center

https://doi.org/10.1017/qua.2023.58 Published online by Cambridge University Press

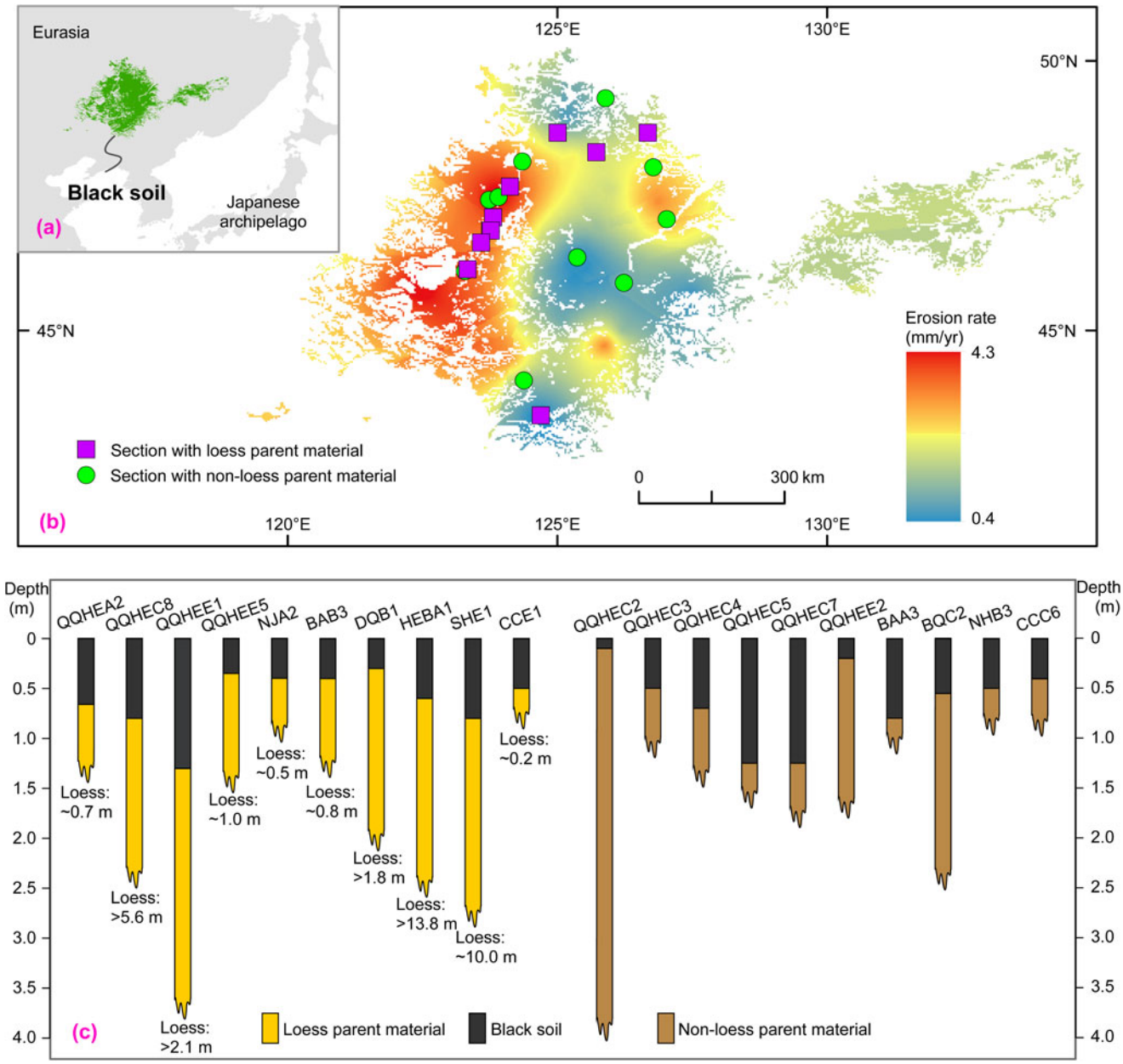


Figure 1. Black soil in northeast China (**a**), contour maps of the erosion rate with locations of the 20 soil sections (**b**), and lithology of black soil sections with loess and non-loess parent materials in the region (**c**). Distribution of black soil in northeast China is modified from ISRIC—World Soil Information (https://files.isric.org/public/soter). Detailed information about these soil sections is presented in Table 1.

Rodrigo-Comino et al., 2018). Measurements from soil plots in eastern Spain revealed that the parent material largely determines the regional erosion rate (Cerdà, 1999, 2002). For example, in the Mediterranean region, soil erosion rates in the marls and colluvial plots were 87.7 and 4.35 Mg/ha/yr, respectively, indicating that soils with the marl as their parent material have a higher erodibility (Rodrigo-Comino et al., 2018). Thus, factors associated with the formation of black soil, especially the inheritance of parent materials, are required for the systematic evaluation of soil erodibility on a large scale.

To date, the effects of parent materials on soil erodibility have not been evaluated on a large scale owing to the absence of an effective indicator that truly mirrors the inheritance of parent materials. Ferromagnetic materials with fine particle sizes continuously accumulate during pedological processes, increasing soil magnetic susceptibility (Liu et al., 2012b). Once soils are eroded, the soil structure is destroyed, leading to fine particulate matter being washed away, further enhancing soil erodibility. This reveals that the eroded soils fail to protect the ferromagnetic materials absorbed by fine particulate matter from leaching. Considering the variations in ferromagnetic materials during pedological processes and excluding the effects of climatic factors, changes in frequency magnetic susceptibility (χ_{fd}, reflecting the amount of fine size ferromagnetic materials; Liu et al., 2012b) could indicate soil erodibility on a regional scale.

In this study, we analysed the χ_{fd} of samples from the black soil horizon of soil sections with loess parent materials and non-loess parent materials, covering an area of severe and slight erosion in

https://doi.org/10.1017/qua.2023.58 Published online by Cambridge University Press

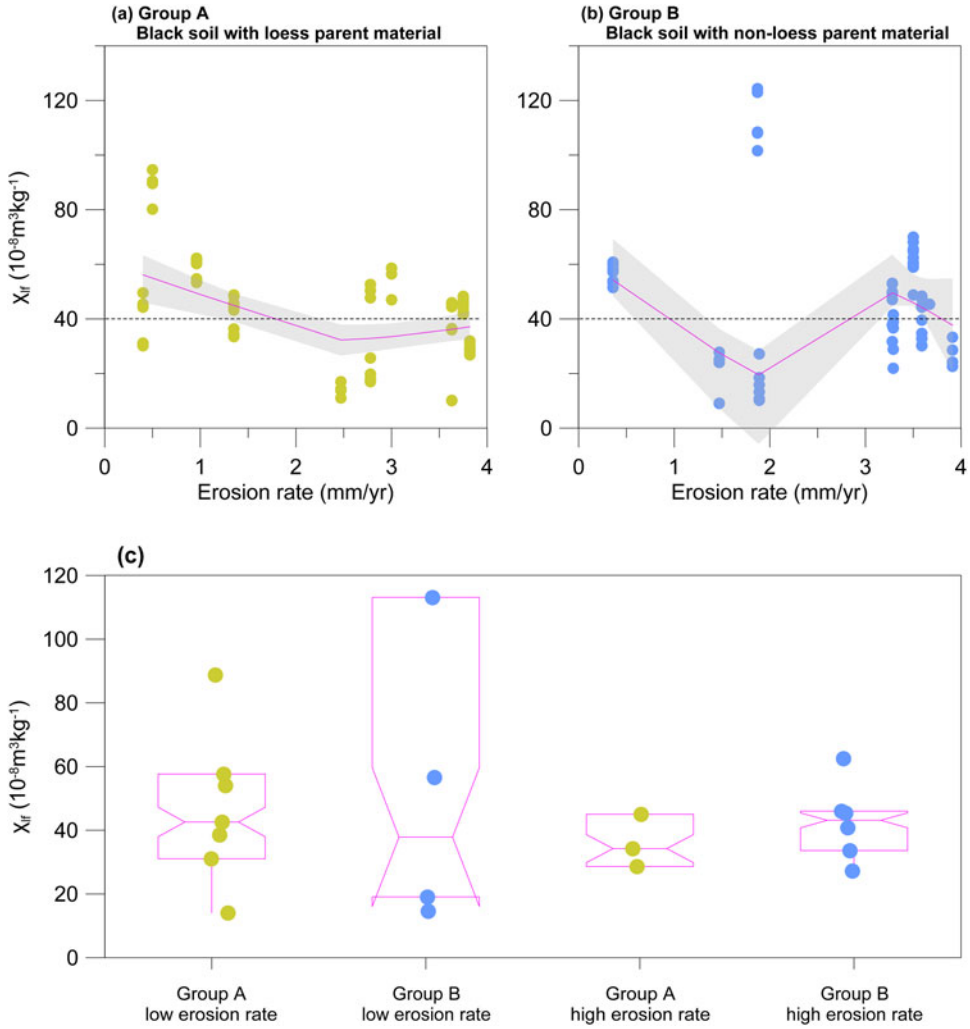


Figure 2. Variations in low-frequency magnetic susceptibility (χ_{lf}) of black soils with (**a**) loess (group A) and (**b**) non-loess (group B) parent materials with increasing erosion rate in northeast China, and (**c**) box plots of χ_{lf} for both groups with low (≤3 mm/yr) and high (>3 mm/yr) erosion rates. The raw data were curve fitted with a locally weighted scatter plot smoothing model. The solid line is the best-fit line, and the colour-filled area shows the 95% confidence level.

northeast China. These data were used to compare variations in the ferromagnetic materials of black soil with different parent materials. In addition, the total organic carbon (TOC) content and stable carbon isotope composition of the bulk organic matter ($\delta^{13}C_{org}$) for selected samples were investigated to indirectly determine the relationship between changes in χ_{fd} and soil erosion. Our principal aim was to determine the effects of parent materials on the erodibility of black soil in northeast China.

METHODS

Study area

The area occupied by black soil in northeast China is geographically located in eastern Eurasia (Fig. 1a), especially in the Songnen, Sanjiang, Greater Khingan Range piedmont, and Liaohe Plains. The modern climate of the region is dominated by a continental monsoon climate that prevails in the cold temperate zone of the Northern Hemisphere. The land–sea thermal contrast in the region is weaker than that in the low latitudes of East Asia. The modern climate is marked by a longer interval of cold and dry conditions in winter and a shorter interval of warm and humid conditions in summer. In the region, the mean annual temperature is in the range of −1°C and 5°C, with the distributions showing a northward-decreasing trend; the mean annual precipitation is from 350 mm to 600 mm, with a decreasing trend from east to west. Precipitation from July to August contributes to 80–90% of the total annual precipitation (Ren et al., 1985). In addition, black soil that developed during the Holocene covers a large area of the region (Cui et al., 2021). The slope angle of the region is from 0° to 5°. The main vegetation types in the region are meadow steppe (Gao et al., 2023), planted poplar, and crops (e.g., corn and soybean).

Sampling

Twenty Holocene soil sections (QQHEA2, QQHEC2, QQHEC3, QQHEC4, QQHEC5, QQHEC7, QQHEC8, QQHEE1, QQHEE2, QQHEE5, NJA2, BAA3, BAB3, DQB1, HEBA1, SHE1, BQC2, NHB3, CCC6, and CCE1) in study areas were used to analyse the χ_{fd} for 142 samples (Table 1), which covered an area of severe and slight erosion (Fig. 1b). Thirty-two samples were selected from five soil profiles (QQHEE1, QQHEC2, BAB3, DQB1, and SHE1) to measure TOC content and $\delta^{13}C_{org}$. All samples were

https://doi.org/10.1017/qua.2023.58 Published online by Cambridge University Press

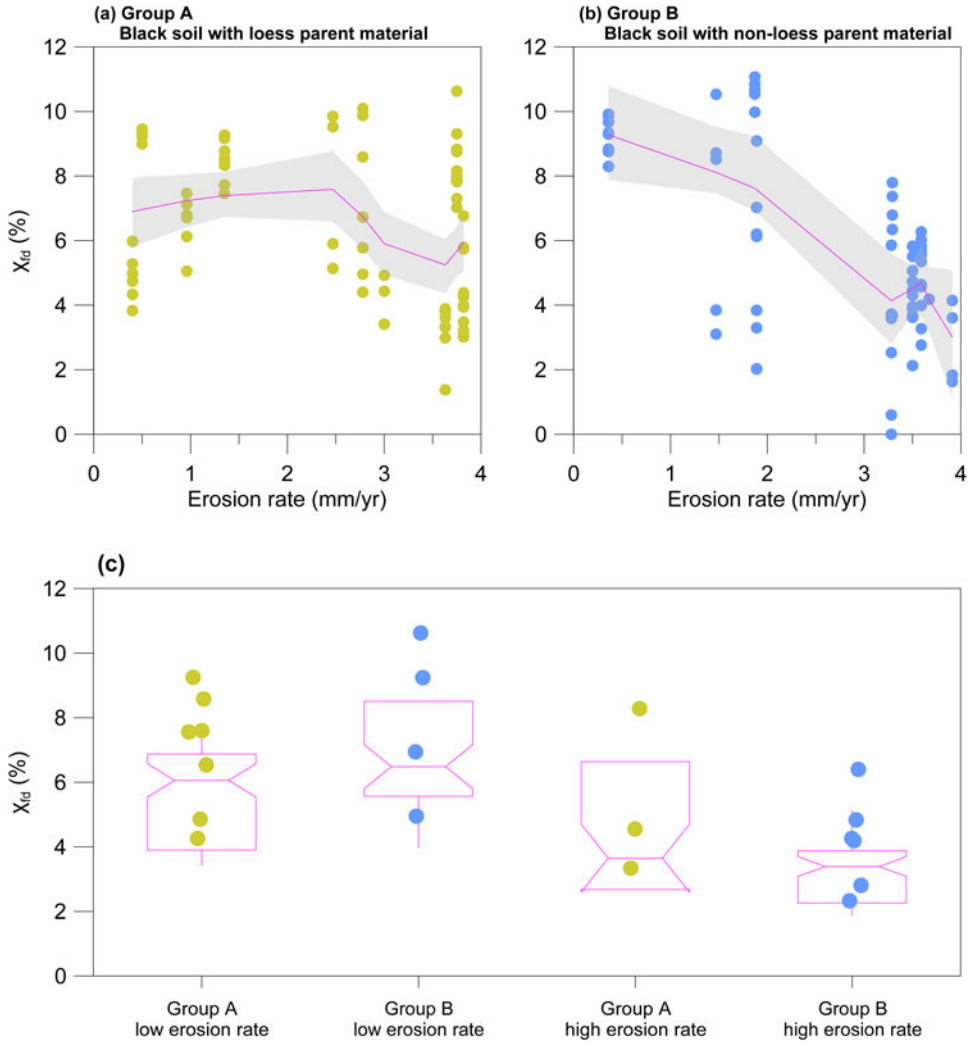


Figure 3. Variations in frequency magnetic susceptibility (χ_{fd}) of black soil with (**a**) loess (group A) and (**b**) non-loess (group B) parent materials with increasing erosion rate in northeast China, and (**c**) box plots of χ_{fd} for both groups with low (≤3 mm/yr) and high (>3 mm/yr) erosion rates. The raw data were curve fitted with a locally weighted scatter plot smoothing model. The solid line is the best-fit line, and the colour-filled area shows the 95% confidence level.

collected at 5–10 cm intervals from 20 sections. The parent materials of black soil from all sections were Quaternary unconsolidated sediments; for example, loess for 10 sections and non-loess materials for the others (Fig. 1c). The non-loess parent materials primarily included fluvial sediments and aeolian sands. The investigation showed that the thickness of the black soil layer for all sections was primarily within the range of 40–90 cm, whereas the minimum was approximately 10 cm (e.g., QQHEC2) and the maximum was approximately 130 cm (e.g., QQHEE1) (Fig. 1c). Additionally, black soil from 20 sections was characterised by a dark black colour (7.5YR5/3–10YR2/1) and relatively high TOC content. Furthermore, the black soils in the region are mature, because the principal soil horizons (O, A, E, B, C, and R) are distinguishable in these sections via a combination of characteristics from both the granular structure and texture of clay and/or silty clay in the A horizon.

Data analysis

A total of 142 samples were collected from 20 soil sections to measure magnetic parameters (Table 1), including low-frequency magnetic susceptibility (χ_{lf}) and high-frequency magnetic susceptibility (χ_{hf}), at the Institute of Geology and Geophysics, Chinese Academy of Sciences. After removal of modern rootlets, χ_{lf} and χ_{hf} were measured on air-dried samples (~10 g) using a Bartington Instruments MS3 magnetic susceptibility meter at frequencies of 0.47 and 4.7 kHz, respectively. Moreover, χ_{fd} was calculated using the formula: $\chi_{fd} = [(\chi_{lf} - \chi_{hf})/\chi_{lf}] \times 100\%$.

Among these sections, 32 samples were selected from five soil profiles (QQHEE1, BAB3, DQB1, SHE1, and QQHEC2) to measure TOC content and $\delta^{13}C_{org}$ (Guo et al., 2023). The measurements were conducted at the Institute of Geology and Geophysics, Chinese Academy of Sciences. Modern rootlets were removed from samples (approx. 3 g) and treated with 10% HCl at approximately 25°C for 24 h to eliminate inorganic carbonate. Thereafter, the residues were washed to a near-neutral pH with distilled water and dried at 45°C. Approximately 500 mg of dried sample was combusted for >4 h at 850°C in evacuated sealed quartz tubes in the presence of silver foil and cupric oxide. The carbon isotopic composition of evolved CO_2 was measured using a MAT-253 gas mass spectrometer with a dual-inlet

https://doi.org/10.1017/qua.2023.58 Published online by Cambridge University Press

Table 1. Detailed information about the 20 soil sections and the measured magnetic parameters of 142 samples in the study region.

No.	Sections	Latitude (°N)	Longitude (°E)	Altitude (m)	Parent material	Extracting erosion rate (mm/yr)	Average value of χ_{lf} (10^{-8} m^3/kg)	Average value of χ_{fd} (%)	No. of samples
1	QQHEA2	47.22	123.73	155	Loess	3.82	28.59	4.55	13
2	QQHEC8	46.10	123.29	151	Loess	3.63	34.20	3.34	8
3	QQHEE1	47.48	123.91	152	Loess	3.75	44.99	8.28	13
4	QQHEE5	48.13	124.35	177	Loess	3.00	54.00	4.26	3
5	NJA2	49.31	125.89	156	Loess	0.50	88.73	9.25	4
6	BAB3	48.03	126.78	336	Loess	2.47	14.03	7.60	4
7	DQB1	46.36	125.37	159	Loess	0.40	38.50	4.86	6
8	HEBA1	45.88	126.23	147	Loess	0.96	57.61	6.54	6
9	SHE1	47.06	127.03	179	Loess	2.78	31.04	7.56	8
10	CCE1	44.07	124.38	209	Loess	1.35	42.55	8.58	10
11	QQHEC2	47.10	123.81	158	Non-loess (aeolian sand)	3.67	45.37	4.19	1
12	QQHEC3	46.85	123.75	143	Non-loess (aeolian sand)	3.29	33.58	6.40	5
13	QQHEC4	46.85	123.76	149	Non-loess (aeolian sand)	3.28	45.94	2.33	7
14	QQHEC5	46.63	123.59	152	Non-loess (aeolian sand)	3.50	62.48	4.26	12
15	QQHEC7	46.13	123.33	137	Non-loess (fluvial sediment)	3.59	40.76	4.83	12
16	QQHEE2	47.67	124.12	156	Non-loess (fluvial sediment)	3.91	27.16	2.81	4
17	BAA3	48.67	126.68	303	Non-loess (fluvial sediment)	1.89	14.59	4.95	8
18	BQC2	48.31	125.72	324	Non-loess (fluvial sediment)	1.87	113.08	10.62	5
19	NHB3	48.67	125.01	307	Non-loess (fluvial sediment)	1.47	19.03	6.94	5
20	CCC6	43.43	124.69	193	Non-loess (fluvial sediment)	0.36	56.55	9.24	8

system, and the TOC content of the samples was determined simultaneously.

In addition, Wang et al. (2022) compiled 24 soil sections to quantify the erosion rate of black soil using ^{137}Cs tracing across the occupied area in northeast China. A kriging interpolation method was subsequently used to generate an estimated surface from the measured erosion rates in the region, which provided the extraction erosion rates for the 20 soil sections (Table 1).

RESULTS

Magnetic characteristics of black soil with loess and non-loess parent materials

The χ_{lf} and χ_{fd} are always used to depict the variations in ferromagnetic materials in multiple disciplines (Dearing, 1999; Liu et al., 2012b). Both proxies were used to depict the magnetic characteristics of black soil with loess and non-loess parent materials in northeast China. Our data showed that the values of χ_{lf} (χ_{fd}) of the black soil layer for 20 sections in northeast China (142 samples) are 9.04×10^{-8} to 124.36×10^{-8} m^3/kg (0–11.07%) (Figs. 2 and 3). The average values of χ_{lf} and χ_{fd} of the black soil layer for a single section in northeast China (20 sections in total), presented in Table 1, reveal that the average χ_{lf} values of the black soil layer are 14.03×10^{-8} to 113.08×10^{-8} m^3/kg, with clustered values of 30×10^{-8} to 60×10^{-8} m^3/kg, and the average values of χ_{fd} of the black soil layer are 2.33–10.62%.

Further investigation revealed that values of χ_{lf} of black soil with loess parent materials (group A) showed a marginal decreasing trend as erosion rate increased (Fig. 2a), whereas the values of χ_{lf} of black soil with non-loess parent materials (group B) exhibited fluctuations (Fig. 2b). Although average values of χ_{lf} for groups A and B are 43.42×10^{-8} m^3/kg and 45.85×10^{-8} m^3/kg, respectively, they fluctuated at an approximate χ_{lf} value of 40×10^{-8} m^3/kg (Fig. 2c). For variations in χ_{fd} with an increasing erosion rate, both groups showed an overall decreasing trend, whereas the decreased range of group B was larger than that of group A (Fig. 3a and b). Compared with χ_{fd} values for group A, the χ_{fd} values for group B were higher at low erosion rates (≤3 mm/yr) and lower at high erosion rates (>3 mm/yr)

https://doi.org/10.1017/qua.2023.58 Published online by Cambridge University Press

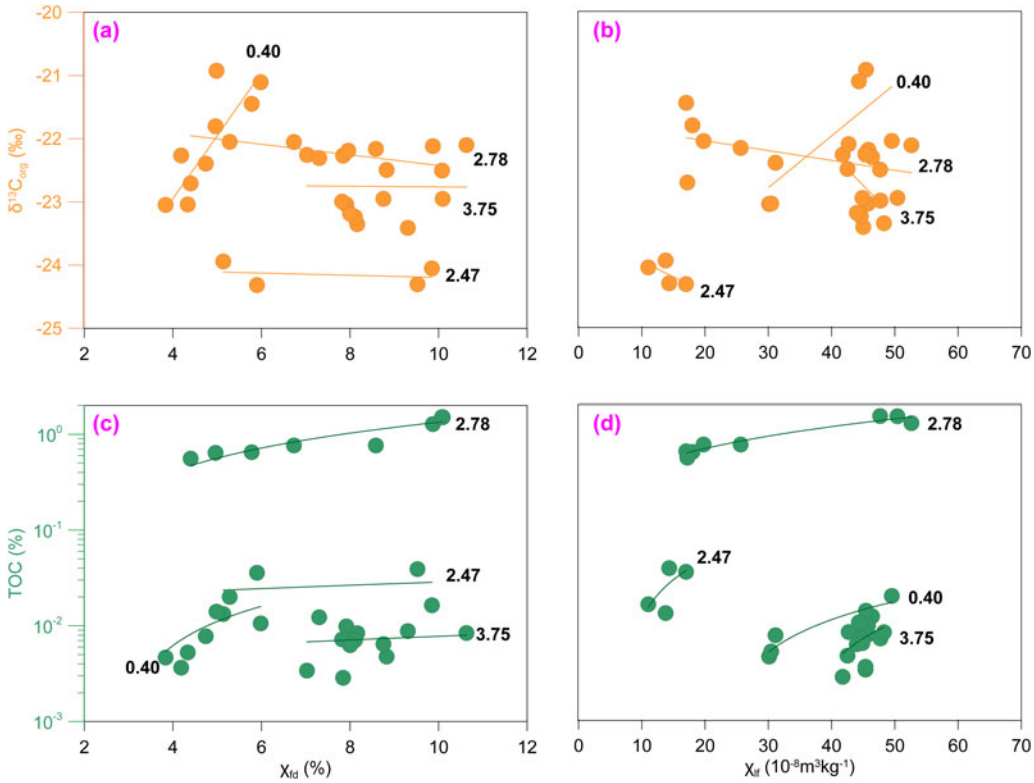


Figure 4. Relationship of (**a and b**) $\delta^{13}C_{org}$ and (**c and d**) total organic carbon (TOC) content with magnetic parameters (frequency magnetic susceptibility, χ_{fd}; and low-frequency magnetic susceptibility, χ_{lf}) for selected sections in northeast China. The values marked in the figure are the erosion rates of the study site (as shown in Table 1). Data from the QQHEE1, BAB3, DQB1, and QQHEC2 sections are provided in Guo et al. (2023).

(Fig. 3c). Overall, the magnetic characteristics of the soil sections with loess and non-loess parent materials were clearly distinguishable through a comparison of χ_{fd} of both groups (Fig. 3).

Variations in TOC content and $\delta^{13}C_{org}$ for selected samples

The values for TOC content and $\delta^{13}C_{org}$ of 32 samples selected from five soil profiles (QQHEE1 [erosion rate = 3.75 mm/yr], QQHEC2 [erosion rate = 3.67 mm/yr], BAB3 [erosion rate = 2.47 mm/yr], DQB1 [erosion rate = 0.40 mm/yr], and SHE1 [erosion rate = 2.78 mm/yr] sections) are presented in Figure 4. The range of $\delta^{13}C_{org}$ values was −24.32‰ to −20.92‰ (Fig. 4a and b). The TOC content was <1%, excluding three samples from SHE1 (Fig. 4c and d). There was a positive correlation between the magnetic parameters (χ_{fd} and χ_{lf}) and TOC content or $\delta^{13}C_{org}$ for the DQB1 (erosion rate = 0.40 mm/yr) section, and weak correlations were observed in other sections (Fig. 4).

DISCUSSION

Contribution of parent materials to erodibility of black soil in northeast China

Soil erodibility is generally estimated using empirical equations based on indicators related to intrinsic soil properties (e.g., soil chemical composition, soil structure, texture, and aggregates) or exogenic erosive forces (e.g., runoff, vegetation, precipitation, and human activities) (Song et al., 2005; Wang et al., 2013). These empirical equations can successfully evaluate soil erodibility within plots under highly controlled conditions based on an experimental design. The effects of parent materials on soil erodibility have been discussed by comparing soil loss rates (Cerdà, 1999, 2002; Rodrigo-Comino et al., 2018). However, the soil loss rate is indistinguishably controlled by parent materials and exogenic erosive forces. Therefore, quantitatively evaluating the contribution of parent materials to soil erodibility on a larger scale has proven challenging.

Existing studies suggest that χ_{lf} is an effective indicator of pedogenesis (Zhou et al., 1990), because higher values indicate the presence of abundant ferromagnetic minerals with continuously accumulated fine size fractions (Dearing, 1999). As eroded soils have less fine particulate matter, low χ_{lf} values occur in some typically eroded locations (Dearing et al., 1986). Additionally, enhanced pedogenesis can result in a quantitative increase in superparamagnetic particles of fine size when the value of χ_{fd} synchronously increases (Liu and Deng, 2009; Liu et al., 2012b). Moreover, the formula $\chi_{fd} = [(\chi_{lf} - \chi_{hf})/\chi_{lf}] \times 100\%$ reveals that χ_{fd} can be used to trace variations in fine size fractions adsorbed in abundant ferromagnetic minerals and superparamagnetic particles for the soil erosion process. Thus, considering the changes in ferromagnetic materials absorbed in fine size fractions in the pedogenic and erosion processes, changes in χ_{lf} and χ_{fd} can serve as reliable indicators of soil erodibility on a regional scale with a close climatic background.

In addition, for eroded soil with fewer fine particles, soil organic matter decomposes to a lower degree, because the higher degree of decomposition requires longer pedogenesis time, and the resultant fractionation would lead to a more positive value of $\delta^{13}C_{org}$. In the study region, $\delta^{13}C_{org}$ increased with the χ_{fd} and χ_{lf} values in the DQB1 section (erosion rate = 0.40 mm/yr),

https://doi.org/10.1017/qua.2023.58 Published online by Cambridge University Press

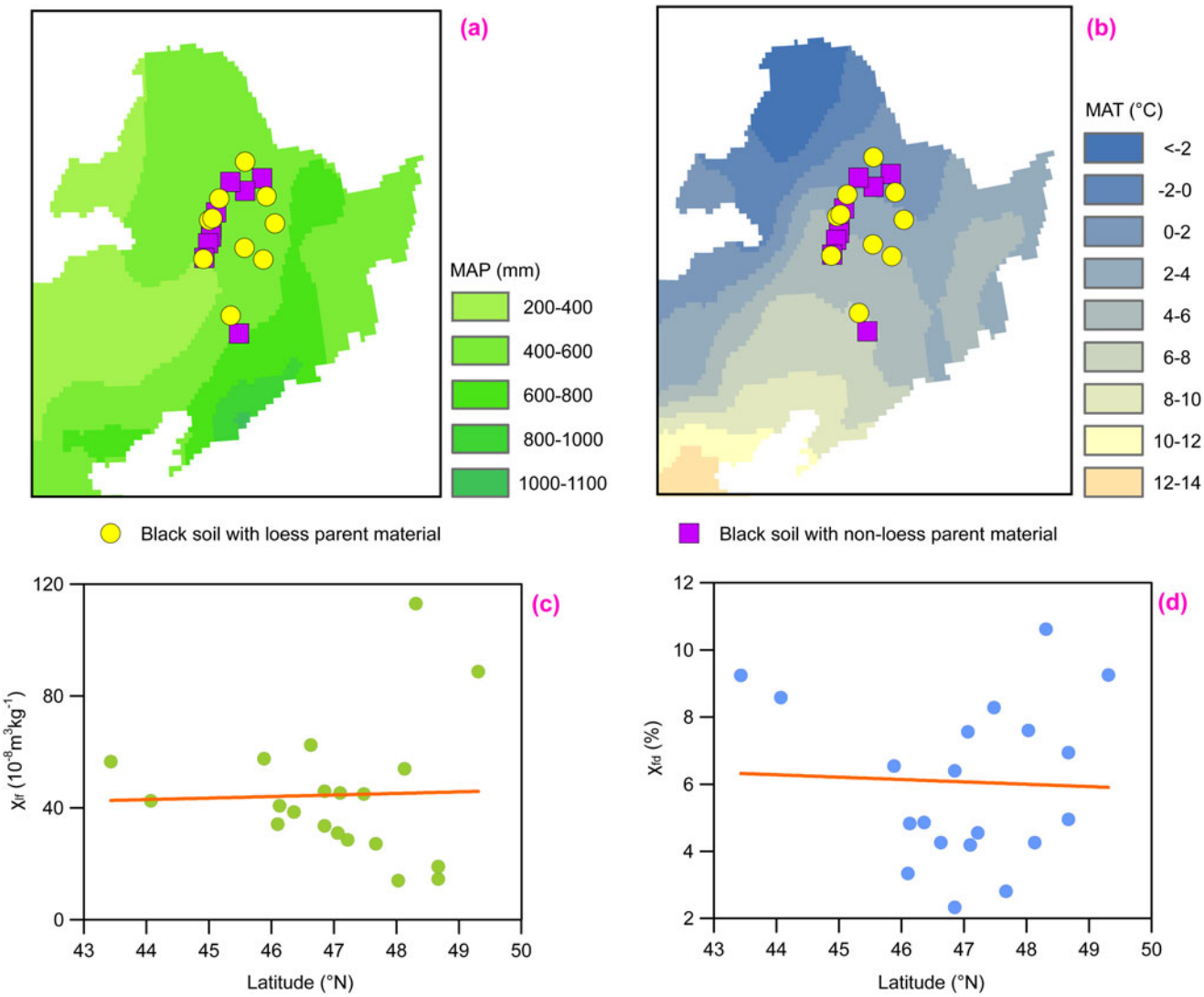


Figure 5. (**a**) Modern mean annual precipitation (MAP) and (**b**) mean annual temperature (MAT) over 30 years (1981–2010) in northeast China, together with variations in average values of (**c**) low-frequency magnetic susceptibility (χ_{lf}) and (**d**) frequency magnetic susceptibility (χ_{fd}) for black soil with latitude. Contour maps of meteorological factors were generated using ArcGIS 10.2, based on long-term climate data provided by the National Meteorological Information Centre of the China Meteorological Administration (http://data.cma.cn).

while weak correlations were observed in other sections (erosion rate = 2–4 mm/yr) (Fig. 4a and b). This suggested that the increases in ferromagnetic minerals and superparamagnetic particles correspond to a high degree of decomposition of soil organic matter, with a positive tendency for $\delta^{13}C_{org}$, supporting the idea that variations in magnetic parameters could depict soil erodibility. Moreover, soil erosion in the Chinese Loess Plateau over the last 60 yr has been effectively monitored by changes in χ_{lf} (Dong et al., 2022).

Climatic and nonclimatic (e.g., inheritance of parent materials) factors can operate together to control changes in ferromagnetic materials during the pedogenic process, further altering the values of soil χ_{lf} and χ_{fd}. Contour maps depicting climatic factors showed that modern mean annual precipitation and temperature of the area covered by the 20 soil sections are from 400 mm to 600 mm and from 0°C to 6°C, respectively (Fig. 5a and b). Although latitudinal variations in temperature were observed, changes in χ_{lf} and χ_{fd} for black soil with latitude were not pronounced (Fig. 5c and d). Thus, the relatively narrow range of climatic factors plays a secondary role in the variations in χ_{lf} and χ_{fd} of the 20 soil sections in the region.

Data analysis showed that χ_{lf} and χ_{fd} is proportional to decreases in erosion rate in the region (Fig. 2 and 3), especially the correlation of χ_{fd} and erosion rate (Fig. 3). This is because fine particulate matter was washed away at a high soil erosion rate, which increased soil erodibility. This suggested that eroded soil fails to protect ferromagnetic materials from runoff. Comparison of black soil with loess (group A) and non-loess (group B) parent materials showed that χ_{lf} fluctuated at approximately 40×10^{-8} m^3/kg (Fig. 2c), and the decreased range of χ_{fd} in group B was larger than that of group A (Fig. 3), revealing that superparamagnetic particles with fine size are more likely eroded in soils formed on non-loess. Consequently, the parent material can be a vital reason for the spatial heterogeneity of the erodibility of black soil in northeast China. In addition, the change in χ_{fd} is narrow in range for black soil with loess parent materials (Fig. 3), suggesting that the erodibility of black soil in the region was relatively low. This conclusion was also

https://doi.org/10.1017/qua.2023.58 Published online by Cambridge University Press

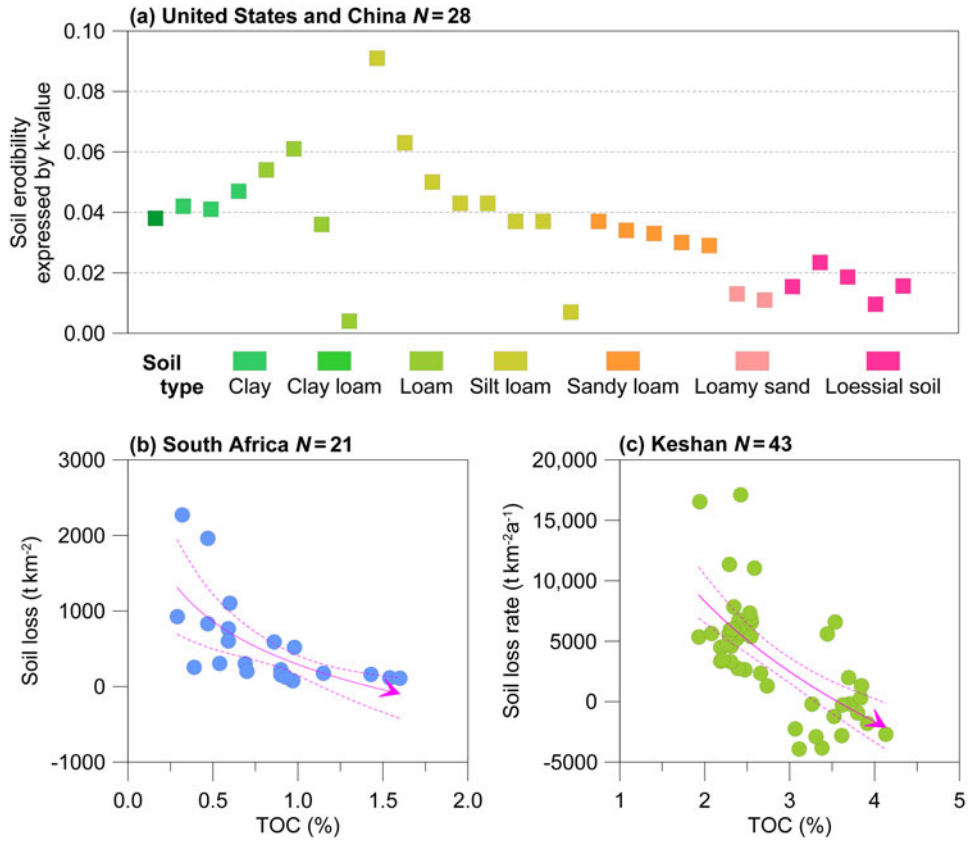


Figure 6. (**a**) Erodibility (expressed by k-value) of soils from the United States and China and (**b and c**) variations in soil loss (or soil loss rate) with the corresponding total organic carbon (TOC) content. (**a**) The k-value is calculated using a soil erodibility nomograph, as proposed by Wischmeier et al. (1971). (**b**) soil loss data are from the Ntabelanga area, Eastern Cape Province, South Africa (Parwada and Tol, 2017). (**c**) Soil erosion rates from Keshan County, Heilongjiang Province, China (He et al., 2021). The solid line is the best-fit line, and the dotted lines show the upper and lower 95% confidence limits.

supported by the relatively low erodibility (expressed by the k-value) of loess soil from China compared with data from the United States (Fig. 6a).

Soil organic carbon induced a decrease in erodibility of black soil with loess parent materials in northeast China

Modern geomorphic regimes have revealed that some fragmented landforms and ecological problems promote erosion in regions covered by loess (Fu, 1989; Fu et al., 2006; Wu et al., 2020). The most important environmental features of the Loess Plateau are the crossbar gullies on the surface and vulnerable ecological conditions. In 2021, the area of soil erosion in the Loess Plateau was up to $\sim 2.06 \times 10^5$ km^2, as reported by the *Bulletin of China on Soil and Water Conservation* released by the Ministry of Water Resources of the People's Republic of China. Moreover, the modern riverbed downstream of the Yellow River is above the land, which is the result of a large amount of sediment from the Loess Plateau in the lower reaches with small flow rates. Sediments with relatively coarse particles (e.g., loess) are highly susceptible to erosion. The high erodibility of loess is mismatched with the relatively low erodibility of black soil with loess parent materials in northeast China.

One of the main reasons for the baffling erodibility of loess and black soil with loess parent materials is the difference in soil organic carbon. For carbon migration during the pedogenic process, soil organic carbon is concentrated in the fine-sized fraction (Roose et al., 2006) because of the greater surface area provided by fine particles. Once soils are eroded, the soil aggregate structure is destroyed, resulting in a direct loss of low-density particulate organic carbon (He et al., 2021). Erosion induces the decrease in fine particulate matter (Meyer and Harmon, 1984; Lee and Gill, 2015), including adsorbed soil organic carbon. Therefore, TOC can be used as a large-scale robust early warning indicator of soil degradation (Guo et al., 2023). Variations in soil loss (or soil loss rate) with the corresponding TOC content from South Africa and northeast China show that a high TOC content corresponds to weak soil erosion (Fig. 6b and c), revealing that the addition of soil organic matter can stabilise the soil against erosion on a global scale (Parwada and Tol, 2017). Although the TOC content of section SHE1 (erosion rate = 2.78 mm/yr) was higher than that of the other sections with high and low erosion rates (Fig. 4c and d), the high values were only from one site. Consequently, we speculated that more soil organic carbon could induce a decrease in the erodibility of black soil with loess parent materials.

In practice, soil organic carbon decreases under the pressure of maintaining high grain yields and erosion (as mentioned in the "Introduction"), necessitating sustainable soil management policies to protect black soil in northeast China to maintain a stable level of sustainable food production. Black soil sustains grain growth with abundant precipitation in summer and autumn when excessive deep ploughing destroys the soil aggregate structure and accelerates soil erosion. Excessive deep ploughing should

https://doi.org/10.1017/qua.2023.58 Published online by Cambridge University Press

be avoided during the ploughing season. For winter and spring, both freeze–thaw action and strong winds result in sparse vegetation cover in the region failing to defend wind erosion for surface soil in northeast China, supported by the works of Chepil (1954) and Coote et al. (1988). Consequently, laying straw over the field to protect surface soil from exposure to strong winds is practical during the fallow season.

CONCLUSIONS

A compilation of values of χ_{lf} and χ_{fd} of 142 samples from the black soil horizon of 10 soil sections with loess parent materials and 10 sections with non-loess parent materials was used to investigate the contributions of parent materials to the erodibility of black soil in northeast China. Moreover, the TOC content and $\delta^{13}C_{org}$ values of 32 samples from five selected sections were also measured. The data revealed that the magnetic parameters (χ_{lf} and χ_{fd}) are proportional to the decrease in the erosion rate, primarily owing to the erosion-induced leaching of ferromagnetic materials and superparamagnetic particles absorbed in fine size fractions. Further, χ_{lf} of black soil with loess (group A) and non-loess (group B) parent materials fluctuated at approximately 40×10^{-8} m^3/kg, and the decreased range of χ_{fd} of group B was larger than that of group A. Considering the changes in ferromagnetic materials absorbed in fine size fractions in the pedogenic and erosion processes, the results suggested that superparamagnetic particles with fine sizes are more likely to be eroded in soils formed on non-loess, indicating that the parent material meaningfully contributes to the spatial heterogeneity of the erodibility of black soil in northeast China. A narrow change in χ_{fd} for group A also indicated the relatively low erodibility of black soil with loess parent materials in the region. Compared with loess marked by less soil organic carbon, more soil organic carbon could induce a decrease in the erodibility of black soil with loess parent materials in northeast China. In addition, we suggest that avoiding excessive deep ploughing in summer and autumn and laying straw over the field in winter and spring should be executed promptly to protect black soil from further erosion, thereby ensuring future food security.

Acknowledgments. This study was supported by the National Natural Science Foundation of China (42007282 and 42077409) and the Key Research Program of the Institute of Geology & Geophysics, Chinese Academy of Sciences (IGGCAS-201905).

REFERENCES

Cerdà, A., 1999. Parent material and vegetation affect soil erosion in Eastern Spain. *Soil Science Society of America Journal* **63**, 362–368.

Cerdà, A., 2002. The effect of season and parent material on water erosion on highly eroded soils in eastern Spain. *Journal of Arid Environments* **52**, 319–337.

Chepil, W.S., 1954. Seasonal fluctuations in soil structure and erodibility of soil by wind. *Soil Science Society of America Journal* **18**, 13–16.

Chesworth, W., 1973. The parent rock effect in the genesis of soil. *Geoderma* **10**, 215–225.

Coote, D.R., Malcolm, C.A., Wall, G.J., Dickinson, W.T., Rudra, R.P., 1988. Seasonal variation of erodibility indices based on shear strength and aggregate stability in some Ontaril soils. *Canadian Journal of Soil Science* **68**, 405–416.

Cui, J.Y., Guo, L.C., Chen, Y.L., Wang, H., Yang, S.L., Xiong, S.F., 2021. Spatial distribution of ^{14}C age and depth of mollisol sections in the Songnen Plain during the Holocene. [In Chinese with English abstract.] *Quaternary Sciences* **41**, 1332–1341.

Dearing, J.A., 1999. *Environmental Magnetic Susceptibility Using the Bartington MS2 System*. Bartington Instruments, Oxford.

Dearing, J.A., Morton, R.I., Price, T.W., Foster, I.D.L., 1986. Tracing movements of topsoil by magnetic measurements: two case studies. *Physics of the Earth and Planetary Interiors* **42**, 93–104.

Dong, H.M., Song, Y.G., Chen, L.M., Liu, H.F., Fu. X.F., Xie, M.P., 2022. Soil erosion and human activities over the last 60 years revealed by magnetism, particle size and minerals of check dams sediments on the Chinese Loess Plateau. *Environmental Earth Sciences* **81**, 162.

[FAO] Food and Agriculture Organization of the United Nations, 2022. *Global Status of Black Soils*. Rome. https://doi.org/10.4060/cc3124en

Fu, B.J., 1989. Soil erosion and its control in the loess plateau of China. *Soil Use and Management* **5**, 76–82.

Fu, B.J., Zhang, Q.J., Chen, L.D., Zhao, W.W., Gulinck, H., Liu, G.B., Yang, Q.K., Zhu, Y.G., 2006. Temporal change in land use and its relationship to slope degree and soil type in a small catchment on the Loess Plateau of China. *Catena* **65**, 41–48.

Gao, G.Z., Wang, M.L., Li, D.H., Li, N.N., Wang, J.Y., Niu, H.H., Meng, M., Liu, Y., Zhang, G.H., Jie, D.M., 2023. Phytolith evidence for changes in the vegetation diversity and cover of a grassland ecosystem in Northeast China since the mid-Holocene. *Catena* **226**, 107061.

Gong, Z.T., Zhang, G.L., Chen, Z.C., 2007. *Pedogenesis and Soil Taxonomy*. China Agriculture Press, Beijing.

Guo, L.C., Xiong, S.F., Chen, Y.L., Cui, J.Y., Yang, S.L., Wang, H., Wang, Y.D., Ding, Z.L., 2023. Total organic carbon content as an early warning indicator of soil degradation. *Science Bulletin* **68**, 150–153.

He, Y.X., Zhang, F.B., Yang, M.Y., 2021. Effects of soil erosion on organic carbon fractions in black soils in sloping farmland of northeast China using ^{137}Cs tracer measurements. [In Chinese with English abstract.] *Transactions of the Chinese Society of Agricultural Engineering* **37**, 60–68.

Kong, T.W., Liu, B.H., Henderson, M., Zhou, W.Y., Su, Y.H., Wang, S., Wang, L.G., Wang, G.B., 2022. Effects of shelterbelt transformation on soil aggregates characterization and erodibility in China black soil farmland. *Agriculture* **12**, 1917.

Lee, J.A., Gill, T.E., 2015. Multiple causes of wind erosion in the Dust Bowl. *Aeolian Research* **19**, 15–36.

Liu, Q.S., Deng, C.L., 2009. Magnetic susceptibility and its environmental significances. [In Chinese with English abstract.] *Chinese Journal of Geophysics* **52**, 1041–1048.

Liu, Q.S., Roberts, A.P., Larrasoaña, J.C., Banerjee, S.K., Guyodo, Y., Tauxe, L., Oldfield, F., 2012b. Environmental magnetism: principles and applications. *Review of Geophysics* **50**, RG4002.

Liu, X.B., Burras, C.L., Kravchenko, Y.S., Duran, A., Huffman, T., Morras, H., Studdert, G., Zhang, X.Y., Cruse, R.M., Yuan, X.H., 2012a. Overview of Mollisols in the world: distribution, land use and management. *Canadian Journal of Soil Science* **92**, 383–402.

Liu, X.B., Zhang, S.L., Zhang, X.Y., Ding, G.W., Cruse, R.M., 2011. Soil erosion control practices in northeast China: a mini-review. *Soil & Tillage Research* **117**, 44–48.

Meyer, L.D., Harmon, W.C., 1984. Susceptibility of agricultural soils to interrill erosion. *Soil Science Society of America Journal* **48**, 1152–1157.

Osher, L.J., Buol, S.W., 1998. Relationship of soil properties to parent material and landscape position in eastern Madre de Dios, Peru. *Geoderma* **83**, 143–166.

Parwada, C., Tol, J.V., 2017. Soil properties influencing erodibility of soils in the Ntabelanga area, Eastern Cape Province, South Africa. *Acta Agriculturae Scandinavica, Section B—Soil & Plant Science* **67**, 67–76.

Ren, M.E., Yang, R.Z., Bao, H.S., 1985. *An Outline of China's Physical Geography*. Foreign Languages Press, Beijing.

Rodrigo-Comino, J., Novara, A., Gyasi-Agyei, Y., Terol, E., Cerdà, A., 2018. Effects of parent material on soil erosion within Mediterranean new vineyard plantations. *Engineering Geology* **246**, 255–261.

Roose, E.J., Lal, R., Feller, C., Barthès, B., Stewart, B.A., 2006. *Soil Erosion and Carbon Dynamics*. CRC Press, Boca Raton, FL.

Song, Y., Liu, L.Y., Yan, P., Cao, T., 2005. A review of soil erodibility in water and wind erosion research. *Journal of Geographical Sciences* **15**, 167–176.

Wang, B., Zheng, F.L., Römkens, M.J.M., Darboux, F., 2013. Soil erodibility for water erosion: a perspective and Chinese experiences. *Geomorphology* **187**, 1–10.

https://doi.org/10.1017/qua.2023.58 Published online by Cambridge University Press

Wang, H., Yang, S.L., Wang, Y.D., Gu, Z.Y., Xiong, S.F., Huang, X.F., Sun, M.M., *et al.*, 2022. Rates and causes of black soil erosion in northeast China. *Catena* **214**, 106250.

Wang, Y., Yang, M.Y., Liu, P.L., 2010. Contribution partition of water and wind erosion on cultivated slopes in northeast black soil region of China. [In Chinese with English abstract.] *Journal of Nuclear Agricultural Sciences* **24**, 790–795.

Wei, D., Meng, K., 2017. *Black Soil of Northeast China*. [In Chinese.] China Agriculture Press, Beijing.

Wischmeier, W.H., Johnson, C.B., Cross, B.V., 1971. A soil erodibility nomograph for farmland and construction sites. *Journal of Soil and Water Conservation* **26**, 189–193.

Wu, X.T., Wei, Y.P., Fu, B.J., Wang, S., Zhao, Y., Moran, E.F., 2020. Evolution and effects of the social-ecological system over a millennium in China's Loess Plateau. *Science Advances* **6**, eabc0276.

Xu, X.Z., Xu, Y., Chen, S.C., Xu, S.G., Zhang, H.W., 2010. Soil loss and conservation in the black soil region of northeast China: a retrospective study. *Environmental Science & Policy* **13**, 793–800.

Yang, X.M., Zhang, X.P., Deng, W., Fang, H.J., 2003. Black soil degradation by rainfall erosion in Jilin, China. *Land Degradation & Development* **14**, 409–420.

Zhou, L.P., Oldfield, F., Wintle, A.G., Robinson, S.G., Wang, J.T., 1990. Partly pedogenic origin of magnetic variations in Chinese loess. *Nature* **346**, 737–739.

https://doi.org/10.1017/qua.2023.58 Published online by Cambridge University Press